

Bending and buckling of a rectangular porous plate

K. Magnucki[†]

*Institute of Applied Mechanics, Poznan University of Technology, ul. Piotrowo 3,
PL. 60-965 Poznan, Poland
Institute of Rail Vehicles "TABOR", ul. Warszawska 181, PL. 61-055 Poznan, Poland*

M. Malinowski[‡]

*Institute of Mechanical Engineering and Machine Operation, University of Zielona Gora,
Zielona Gora, Poland*

J. Kasprzak^{‡†}

Institute of Applied Mechanics, Poznan University of Technology, Poznan, Poland

(Received July 5, 2005, Accepted February 14, 2006)

Abstract. A rectangular plate made of a porous material is the subject of the work. Its mechanical properties vary continuously on the thickness of a plate. A mathematical model of this plate, which bases on nonlinear displacement functions taking into account shearing deformations, is presented. The assumed displacement field, linear geometrical and physical relationships permit to describe the total potential energy of a plate. Using the principle of stationarity of the total potential energy the set of five equilibrium equations for transversely and in-plane loaded plates is obtained. The derived equations are used for solving a problem of a bending simply supported plate loaded with transverse pressure. Moreover, the critical load of a bi-axially in-plane compressed plate is found. In both cases influence of parameters on obtained solutions such as a porosity coefficient or thickness ratio is analysed. In order to compare analytical results a finite element model of a porous plate is built using system ANSYS. Obtained numerical results are in agreement with analytical ones.

Keywords: non-homogeneous plate; elastic buckling; rectangular plate.

1. Introduction

Plates of changing thickness properties are widely used, from furniture industries to aerospace projects. The simplest example of such a construction is a laminated plate (laminated) which is built of few layers made of materials of different mechanical properties. A sandwich plate is another particular example of such constructions. It is composed of two stiff outer layers (facings) and a light core placed between the facings. Mechanical properties of laminates vary discretely on thickness. More advanced examples of

[†]Professor Eng., Corresponding author, E-mail: Krzysztof.Magnucki@put.poznan.pl

[‡]PhD Eng.

^{‡†}MSc, PhD Student

non-homogeneous plates are made of porous or graded materials. In these structures mechanical properties vary continuously on thickness of plate. An extensive article describing the manufacturing, testing and applications of such materials is the work of Banhart (2001) that contains more than 300 references. Another example of a work devoted to porous materials is the monograph of Mielniczuk (2000).

The simplest, widely used approach to modelling plates made of non-homogeneous materials is using Kirchhoff-Love's hypothesis for describing the displacement field and taking into account modified forms of stiffness coefficients. This way of modelling was used for example in the monograph of Ambartsumian (1987). Advantages of this approach are simplicity and ability to use solutions derived for homogeneous plates, which may be found in Wozniak (2001) the rich monograph devoted to plates and shells. The main disadvantage is neglecting shear forces and displacements, which restrict using this approach to thin plates without rapid changes of mechanical properties.

Classical Laminated Plate Theory (CLPT) is based on the above assumptions. Its description may be found in Jones (1975), where authors also deal with optimization of multilayered structures. The same approach and its extension on First Shear Deformation Theory are presented in Vinson (1999) and in the extensive monograph of Reddy (2004).

In order to overcome the aforementioned difficulties a lot of higher order hypotheses, which include shearing, have been formulated. An example of a monograph devoted to this problem is the work of Wang *et al.* (2000), where authors presented not only their own solutions but also a review of previous attempts to model beams and plates. A thorough review of theories, including zig-zag ones, used for modelling multilayered plates and rich bibliography may be found in the work of Carrera (2000), review articles of Carrera (2001, 2003) devoted also to shells. A comparison of theories used for modelling compressed and bent multilayered composite plates is presented in Chattopadhyay and Gu (1996), Idlbi *et al.* (1997) and in the work of Noor and Malik (2000), where authors considered also thermal loading.

Computational models for sandwich panels and shells are discussed by Noor *et al.* (1996).

There have already been attempts to model the mechanics of structures of changing properties. Their results are papers devoted to porous beams Magnucki and Stasiewicz (2004a), and Magnucki and Stasiewicz (2004b). This work is an extension of the ideas presented in the above papers to porous plates.

2. Basic relations and differential equations of equilibrium

The subject of the work is a rectangular porous plate the dimensions of which are length a , width b and thickness t (Fig. 1).

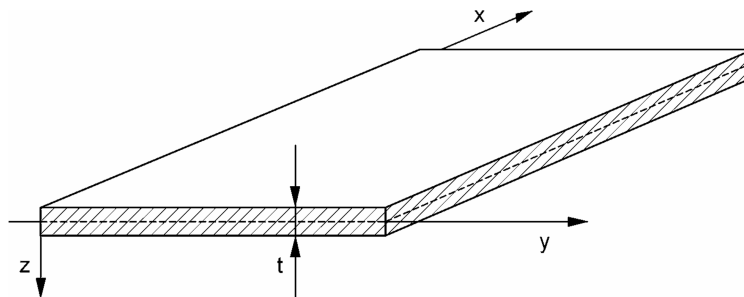


Fig. 1 Model of a plate

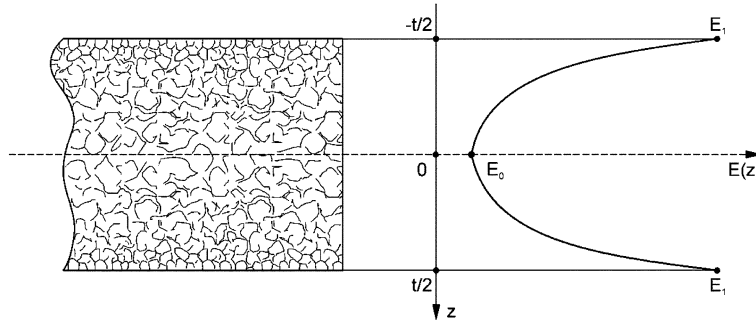


Fig. 2 The variability of Young's modulus on the thickness of a plate

Mechanical properties of a plate vary on the thickness of a plate and depend on porosity of a material (Fig. 2). The functions expressing the change of moduli of elasticity are the same as those assumed in the works of Magnucki and Stasiewicz (2004a, 2004b) and has a form

$$E(z) = E_1[1 - e_0 \cos(\pi \zeta)], \quad G(z) = G_1[1 - e_0 \cos(\pi \zeta)] \tag{1}$$

where:

$$e_0 = 1 - \frac{E_0}{E_1} = 1 - \frac{G_0}{G_1} \text{ - the porosity coefficient of a plate, } G_j = \frac{E_j}{2(1 + \nu)}, \quad j = 0, 1,$$

E_0, G_0, E_1, G_1 - moduli of elasticity for $\zeta=0$ and $\zeta=\pm\frac{1}{2}$,

$\zeta = \frac{z}{t}$ - the dimensionless coordinate, ν - Poisson's ratio.

A flat plane of a cross-section perpendicular to the mid-plane of a plate before deformation changes after deformation to a surface, which is perpendicular only to the outer planes of a plate ($z = \pm t/2$). This hypothesis of deformation is presented in Fig. 3.

The displacement field of the considered plate is defined on a basis of the previous works of Magnucki (2003), Magnucki and Stasiewicz (2004) and have the following form:

$$u(x, y, z) = -t \left\{ \zeta \frac{\partial w}{\partial x} - \frac{1}{\pi} [\psi_1(x, y) \sin(\pi \zeta) + \psi_2(x, y) \sin(2\pi \zeta) \cos^2(\pi \zeta)] \right\} \tag{2}$$

$$v(x, y, z) = -t \left\{ \zeta \frac{\partial w}{\partial y} - \frac{1}{\pi} [\phi_1(x, y) \sin(\pi \zeta) + \phi_2(x, y) \sin(2\pi \zeta) \cos^2(\pi \zeta)] \right\} \tag{3}$$

$$w(x, y) \text{ - deflection of a plate (the mid-plane)} \tag{4}$$

and components of strain state – geometrical relations are included in Annex.

The principle of stationarity of the total potential energy of a plate

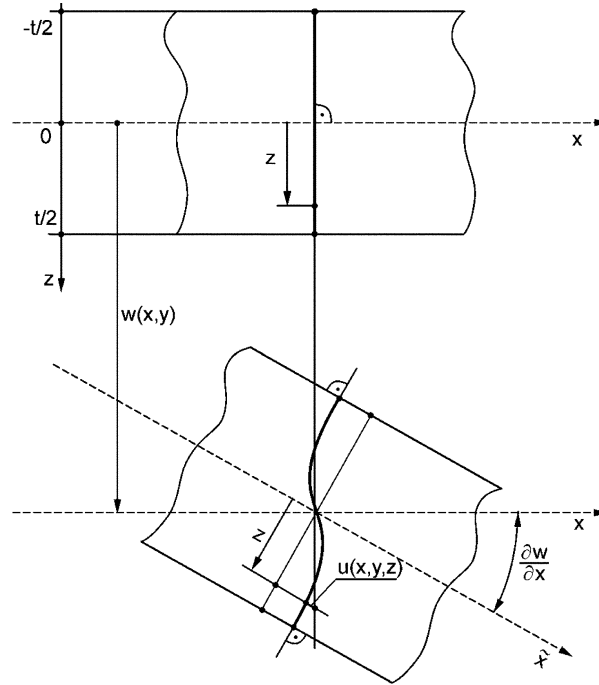


Fig. 3 Displacements of a cross section of a plate wall

$$\delta(U_\varepsilon - W) = 0 \quad (5)$$

where:

$$U_\varepsilon = \frac{t}{2} \iint_{\Omega} \int_{-1/2}^{1/2} (\sigma_x \varepsilon_x + \sigma_y \varepsilon_y + \tau_{xy} \gamma_{xy} + \tau_{xz} \gamma_{xz} + \tau_{yz} \gamma_{yz}) dx dy d\zeta - \text{the elastic strain energy,}$$

$$W = \iint_{\Omega} \left[p \cdot w + \frac{1}{2} N_x \left(\frac{\partial w}{\partial x} \right)^2 + \frac{1}{2} N_y \left(\frac{\partial w}{\partial y} \right)^2 \right] dx dy - \text{the work of load.}$$

p [MPa] – transverse pressure,

N_x, N_y [N/mm] – intensity of in-plane load.

Taking into account linear physical relations (Hooke law) and Eq. (1), the elastic strain energy may be written in the form

$$U_\varepsilon = \frac{E_1 t}{2(1-\nu^2)} \iint_{\Omega} \int_{-1/2}^{1/2} \left[1 - e_0 \cos(\pi \zeta) \right] \left[\varepsilon_x^2 + 2\nu \varepsilon_x \varepsilon_y + \varepsilon_y^2 + \frac{1-\nu}{2} (\gamma_{xy}^2 + \gamma_{xz}^2 + \gamma_{yz}^2) \right] dx dy d\zeta \quad (6)$$

From the principle of stationarity of the total potential energy of a plate Eq. (5), after integrating over the thickness of plate ($-1/2 \leq \zeta \leq 1/2$) and integrating by parts over the mid-plane a system of five partial differential equations is obtained

$$\begin{aligned} \delta w) \quad & \frac{E_1 t^3}{1-\nu^2} \left[C_1 \nabla^4 w - C_2 \left(\frac{\partial}{\partial x} (\nabla^2 \psi_1) + \frac{\partial}{\partial y} (\nabla^2 \phi_1) \right) - C_3 \left(\frac{\partial}{\partial x} (\nabla^2 \psi_2) + \frac{\partial}{\partial y} (\nabla^2 \phi_2) \right) \right] = \\ & = p - N_x \frac{\partial^2 w}{\partial x^2} - N_y \frac{\partial^2 w}{\partial y^2} \end{aligned} \quad (7)$$

$$\begin{aligned} \delta \psi_1) \quad & C_2 \frac{\partial}{\partial x} (\nabla^2 w) - C_4 \left(\frac{\partial^2 \psi_1}{\partial x^2} + \frac{1-\nu}{2} \frac{\partial^2 \psi_1}{\partial y^2} + \frac{1+\nu}{2} \frac{\partial^2 \phi_1}{\partial x \partial y} \right) + \\ & - C_5 \left(\frac{\partial^2 \psi_2}{\partial x^2} + \frac{1-\nu}{2} \frac{\partial^2 \psi_2}{\partial y^2} + \frac{1+\nu}{2} \frac{\partial^2 \phi_2}{\partial x \partial y} \right) + \frac{1-\nu}{2t^2} (C_7 \psi_1 + C_8 \psi_2) = 0 \end{aligned} \quad (8)$$

$$\begin{aligned} \delta \phi_1) \quad & C_2 \frac{\partial}{\partial y} (\nabla^2 w) - C_4 \left(\frac{\partial^2 \phi_1}{\partial y^2} + \frac{1-\nu}{2} \frac{\partial^2 \phi_1}{\partial x^2} + \frac{1+\nu}{2} \frac{\partial^2 \psi_1}{\partial x \partial y} \right) + \\ & - C_5 \left(\frac{\partial^2 \phi_2}{\partial y^2} + \frac{1-\nu}{2} \frac{\partial^2 \phi_2}{\partial x^2} + \frac{1+\nu}{2} \frac{\partial^2 \psi_2}{\partial x \partial y} \right) + \frac{1-\nu}{2t^2} (C_7 \phi_1 + C_8 \phi_2) = 0 \end{aligned} \quad (9)$$

$$\begin{aligned} \delta \psi_2) \quad & C_3 \frac{\partial}{\partial x} (\nabla^2 w) - C_5 \left(\frac{\partial^2 \psi_1}{\partial x^2} + \frac{1-\nu}{2} \frac{\partial^2 \psi_1}{\partial y^2} + \frac{1+\nu}{2} \frac{\partial^2 \phi_1}{\partial x \partial y} \right) + \\ & - C_6 \left(\frac{\partial^2 \psi_2}{\partial x^2} + \frac{1-\nu}{2} \frac{\partial^2 \psi_2}{\partial y^2} + \frac{1+\nu}{2} \frac{\partial^2 \phi_2}{\partial x \partial y} \right) + \frac{1-\nu}{2t^2} (C_8 \psi_1 + C_9 \psi_2) = 0 \end{aligned} \quad (10)$$

$$\begin{aligned} \delta \phi_2) \quad & C_3 \frac{\partial}{\partial y} (\nabla^2 w) - C_5 \left(\frac{\partial^2 \phi_1}{\partial y^2} + \frac{1-\nu}{2} \frac{\partial^2 \phi_1}{\partial x^2} + \frac{1+\nu}{2} \frac{\partial^2 \psi_1}{\partial x \partial y} \right) + \\ & - C_6 \left(\frac{\partial^2 \phi_2}{\partial y^2} + \frac{1-\nu}{2} \frac{\partial^2 \phi_2}{\partial x^2} + \frac{1+\nu}{2} \frac{\partial^2 \psi_2}{\partial x \partial y} \right) + \frac{1-\nu}{2t^2} (C_8 \phi_1 + C_9 \phi_2) = 0 \end{aligned} \quad (11)$$

where the form of coefficients C_i is presented in Annex.

The system of partial differential Eqs. (7) – (11) is solved in an approximated way by assuming five unknown functions having a form

$$\begin{aligned} w(x, y) &= w_a \cdot \sin \frac{m\pi x}{a} \sin \frac{n\pi y}{b}, \quad m = 1, 2, \dots, \quad n = 1, 2, \dots, \\ \psi_j(x, y) &= \psi_{aj} \cdot \cos \frac{m\pi x}{a} \sin \frac{n\pi y}{b}, \quad \phi_j(x, y) = \phi_{aj} \cdot \sin \frac{m\pi x}{a} \cos \frac{n\pi y}{b}, \quad j = 1, 2 \end{aligned} \quad (12)$$

where:

w_a – the amplitude of deflection, ψ_{aj}, ϕ_{aj} – parameters of functions.

From Eqs. (8), (10) and (9), (11) it is obtained

$$\psi_{a2} = C_{10} \cdot \psi_{a1}, \quad \psi_{a2} = C_{10} \cdot \psi_{a1} \quad (13)$$

where

$$C_{10} = \frac{C_3 C_7 - C_2 C_8}{C_2 C_9 - C_3 C_8}$$

These relations are obtained assuming simplifications specified below

$$C_2 C_5 - C_2 C_4 \cong 0, \quad C_2 C_6 - C_3 C_5 \cong 0, \quad \text{for } 0 \leq e_0 < 1 \quad (14)$$

Remaining two parameters of the functions $\psi_1(x, y)$ and $\phi_1(x, y)$ are expressed in the following way

$$\psi_{a1} = \alpha_1 \cdot \tilde{w}_a, \quad \phi_{a1} = \beta_1 \cdot \tilde{w}_a \quad (15)$$

where $\tilde{w}_a = w_a/t$ is the dimensionless amplitude of deflection and the form of coefficients α_1, β_1 is presented in Annex.

The first Eq. (7) of the system of five equations includes loads. After solving it the deflection of a plate \tilde{w}_a or the critical load $N_{x, KR}$ may be obtained.

3. Strength of a bending porous plate

It is assumed that a porous rectangular plate is loaded with uniformly distributed transverse pressure p_0 [MPa]. From the orthogonalization condition of Galerkin method for Eq. (7)

$$\int_0^a \int_0^b [\Re(x, y) - p_0] \sin \frac{m\pi x}{a} \sin \frac{n\pi y}{b} dx dy = 0 \quad (16)$$

where $\Re(x, y)$ is the left side of this equation, the relative deflection is obtained

$$\tilde{w}_a = \frac{16(1-\nu^2)p_0}{\pi^5 k_0 E_1} \quad (17)$$

where

$$k_0 = \left\{ \pi \left[1 + \left(\frac{a}{b} \right)^2 \right] C_1 \frac{t}{a} - (C_2 + C_3 C_{10}) \left(\alpha_1 + \frac{a}{b} \beta_1 \right) \right\} \left[1 + \left(\frac{a}{b} \right)^2 \right] \left(\frac{t}{a} \right)^3 \text{ and } m = n = 1$$

In particular, when a plate is uniform – isotropic ($e_0 = 0$) and Kirchhoff-Love hypothesis is valid ($\psi_j = \phi_j = 0$), the relative deflection is obtained from Eq. (17) and has a form

$$\tilde{w}_{a,0} = \frac{16}{\pi^6} \frac{a^4 p_0}{D \left[1 + \left(\frac{a}{b} \right)^2 \right]^2 t}, \quad \text{where } D = \frac{Et^3}{12(1-\nu^2)} \quad (18)$$

which coincides with the classical solution presented for example in the monograph of Bažant and Cedolin (1991).

Normal stresses basing on Hooke law are expressed as follows

$$\sigma_x = \frac{E(\zeta)}{1-\nu^2}(\varepsilon_x + \nu\varepsilon_y), \quad \sigma_y = \frac{E(\zeta)}{1-\nu^2}(\varepsilon_y + \nu\varepsilon_x)$$

They have maximum values in the middle of plate ($x = a/2, y = b/2$). Taking into account Eqs. (1), (A1), (A2), (13), (15) and (17) the maximum stresses are equal to:

$$\begin{aligned} \sigma_x &= \frac{16}{\pi^5 k_0} \frac{t}{a} \left\{ \pi^2 \frac{t}{a} \left[1 + \nu \left(\frac{a}{b} \right)^2 \right] \zeta - \left(\alpha_1 + \nu \beta_1 \frac{a}{b} \right) [\sin(\pi\zeta) + C_{10} \sin(2\pi\zeta) \cos^2(\pi\zeta)] \right\} f_e \cdot p_0 \\ \sigma_y &= \frac{16}{\pi^5 k_0} \frac{t}{a} \left\{ \pi^2 \frac{t}{a} \left[\nu + \left(\frac{a}{b} \right)^2 \right] \zeta - \left(\nu \alpha_1 + \beta_1 \frac{a}{b} \right) [\sin(\pi\zeta) + C_{10} \sin(2\pi\zeta) \cos^2(\pi\zeta)] \right\} f_e \cdot p_0 \end{aligned} \quad (19)$$

where

$$f_e = 1 - e_0 \cos(\pi\zeta)$$

A numerical analysis was carried out for the family of rectangular porous plates with the following parameters:

$$\frac{a}{b} = 1; \quad \frac{t}{a} = \frac{1}{10}, \frac{1}{11}, \frac{1}{12}, \frac{1}{13}, \frac{1}{14}, \frac{1}{15}; \quad e_0 = 0.90, 0.99; \quad \nu = 0.3;$$

$$E_1 = 2.05 \cdot 10^5 \text{MPa}; \quad p_0 = 1 \text{MPa}$$

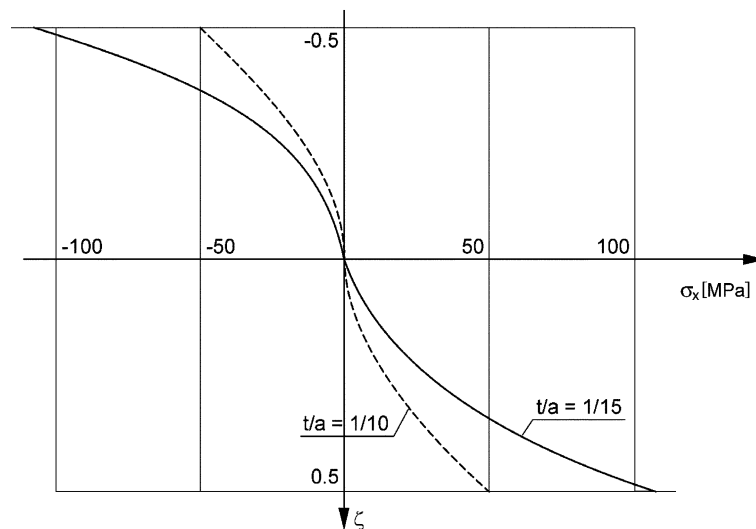


Fig. 4 Normal stresses σ_x [MPa] vs. the thickness of a plate ($e_0 = 0.9$)

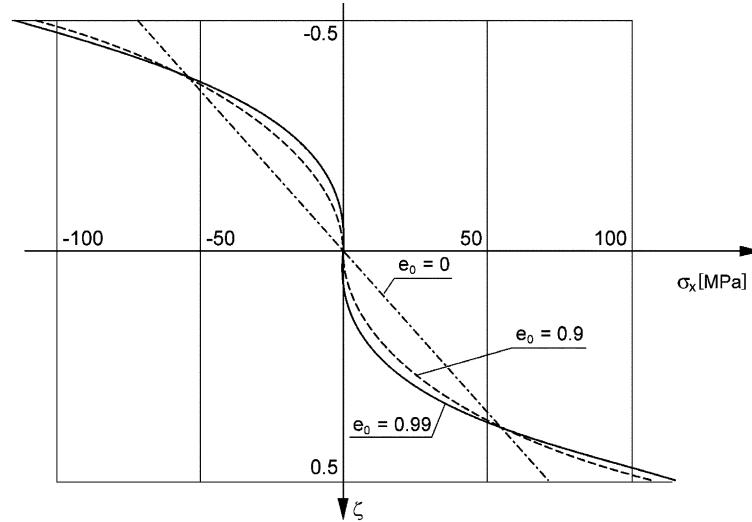


Fig. 5 Normal stresses σ_x [MPa] vs. the thickness of a plate ($t/a = 1/15$)

Graphs of maximum normal stresses σ_x [MPa] that vary on the thickness of square plates $t/a = 1/10$ and $t/a = 1/15$ are presented in Fig. 4.

Graphs of maximum normal stresses σ_x [MPa] that vary on the thickness of square plates ($t/a = 1/15$) for different porosity coefficients $e_0 = 0, 0.9$ and 0.99 are presented in Fig. 5.

4. Critical load of in-plane compressed porous plate

Rectangular porous plate is bi-axially loaded with compressive in-plane forces. Intensity of these loads N_x and N_y is constant on the edges of a plate (Bažant and Cedolin 1991). From the orthogonalization condition of Galerkin method for Eq. (7)

$$\int_0^a \int_0^b \left[\Re(x, \varphi) + N_x \frac{\partial^2 w}{\partial x^2} + N_y \frac{\partial^2 w}{\partial y^2} \right] \sin \frac{m\pi x}{a} \sin \frac{n\pi y}{b} dx dy = 0 \quad (20)$$

where $\Re(x, y)$ is the left side of Eq. (7), the dimensionless critical load is obtained and has a following form

$$f_{x, CR} = (1 - \nu^2) \left(\frac{N_x}{E_1 t} \right)_{CR} = \min_{m, n} \left\{ m \pi \frac{t}{a} \cdot k_1 \frac{1 + k_2^2}{1 + C_{xy} k_2^2} \right\} \quad (21)$$

where

$$k_1 = m \pi \frac{t}{a} (1 + k_2^2) C_1 - (C_2 + C_3 C_{10}) (\alpha_1 + \beta_1 k_2), \quad k_2 = \frac{n a}{m b}, \quad C_{xy} = N_y / N_x$$

Kirchhoff-Love hypothesis is valid, in particular case, when $\psi_j = \phi_j = 0$ and the plate is uniform – isotropic, i.e., $e_0 = 0$. Then, if the plate is compressed only along the x axis the critical load is

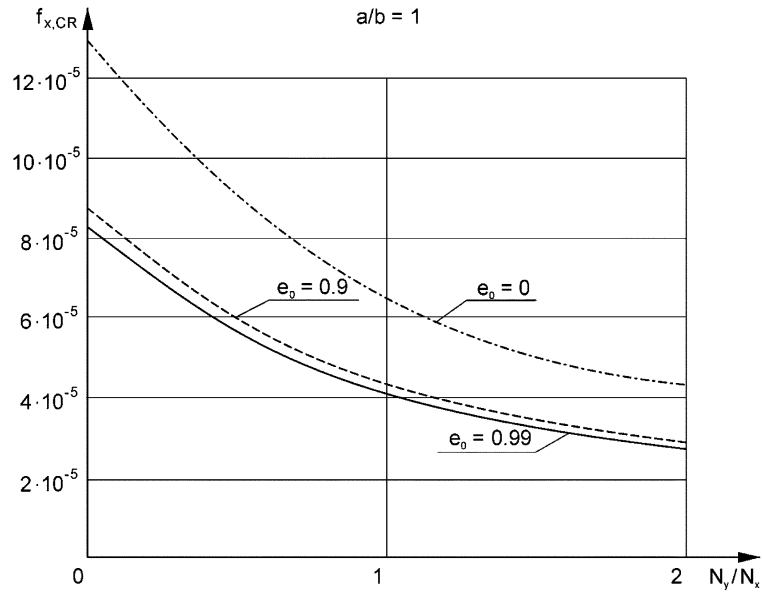


Fig. 6 Dimensionless critical load for a bi-axially compressed plate

obtained from Eq. (21) and has a form

$$N_{x,CR} = \min_m \left\{ \left(\frac{m\pi}{a} \right)^2 \left[1 + \left(\frac{1}{m} \frac{a}{b} \right)^2 \right] \right\} \frac{1}{D}, \quad \text{where } D = \frac{Et^3}{12(1-\nu^2)} \quad (22)$$

which coincides with the classical solution presented for example in the monograph of Bažant and Cedolin (1991).

A numerical analysis was carried out for the family of rectangular porous plates with the following parameters:

$$\frac{a}{b} = \frac{1}{3}, \frac{1}{2}, 1; \quad \frac{t}{a} = \frac{1}{160}; \quad e_0 = 0.90, 0.99; \quad \nu = 0.3; \quad E_1 = 2.05 \cdot 10^5 \text{ MPa}$$

Influence of the ratio of load ($C_{xy} = N_y / N_x$) on the longitudinal critical load ($f_{x,CR}$) is shown in Fig. 6.

5. Numerical tests with the use of FEM analysis

A numerical analysis of an isotropic beam made of a porous material was carried out by Magnucki and Stasiewicz (2004). Deflection and stresses obtained analytically and numerically (FEM) were presented by them.

In the considered problem the FEM analysis of a porous plate was done in ANSYS. A discrete model of a plate was built from finite elements SHELL99, in which 22 layers were defined. The mechanical properties E and ν in the mid-plane of each layer were calculated from Eq. (1).

5.1. Bending of a porous plate

A numerical analysis was carried out for the same group of rectangular porous plates that was used in analytical calculations. The graphs of the normal stresses in the middle cross section of plates obtained from FEM analysis σ_x [MPa] for $a/b = 1$ with a thickness ratio $t/a = 1/10, 1/15$ and porosity coefficient $e_0 = 0.99$ and $e_0 = 0.9$ are presented in Figs. 7 and 8.

It may be seen in the figures that stresses vary linearly on the thickness of each layer. The maximum stresses in the outer layers are equal to 101.17 MPa for $t/a = 1/15$; $e_0 = 0.90$ and 107.0 MPa for $t/a = 1/15$; $e_0 = 0.99$. Obtained results are consistent with the analytical calculations.

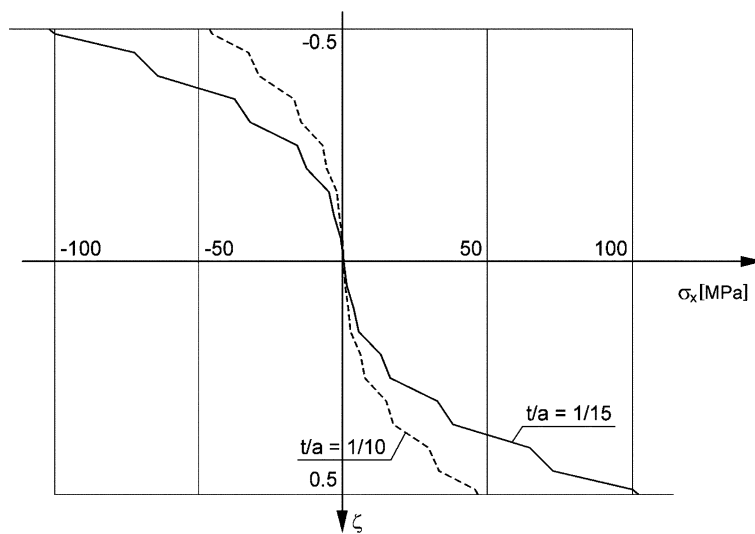


Fig. 7 The normal stress for the middle cross section of square plates ($e_0 = 0.99$)

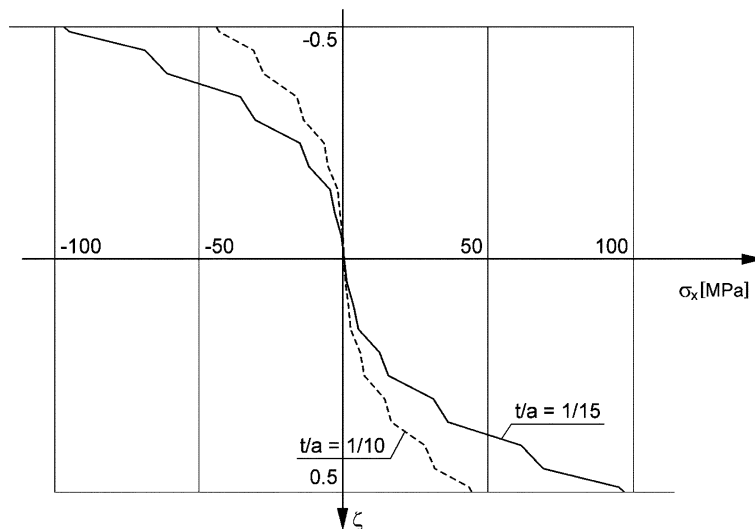


Fig. 8 The normal stress for the middle cross section of square plates ($e_0 = 0.90$)

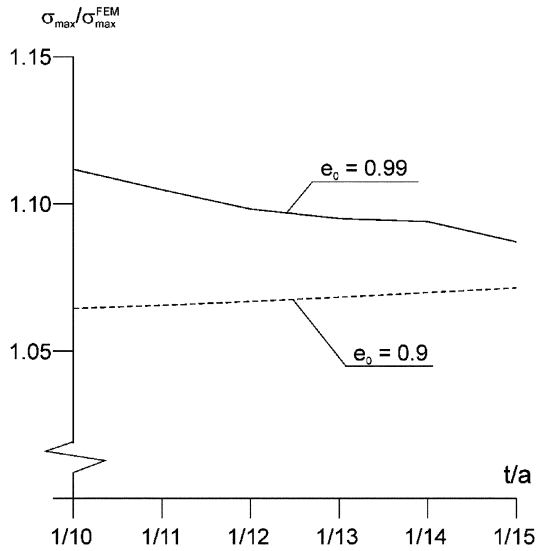


Fig. 9 The ratio of the normal stress of square plates

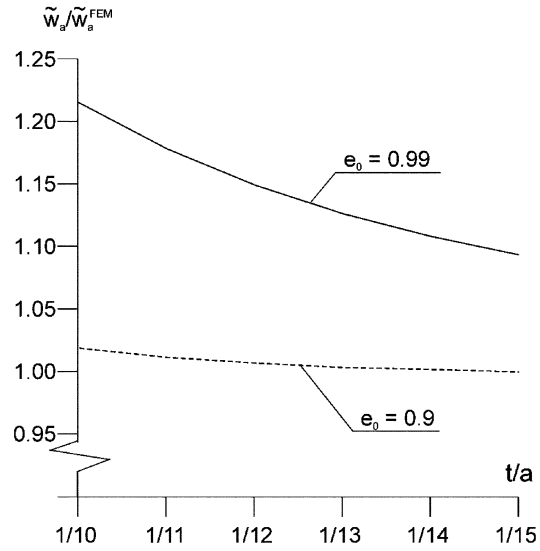


Fig. 10 The ratio of the dimensionless deflection of square plates

The ratio of analytical results to FEM results are shown in Fig. 9. Its maximum value is equal to 1.112 for $t/a = 1/10$; $e_0 = 0.99$ and 1.072 for $t/a = 1/15$; $e_0 = 0.90$. The number of layers in a FEM model should be increased if more accurate numerical results are needed.

In order to compare the results the ratio of analytically obtained relative deflection to numerically obtained one is shown in Fig. 10. Its maximum value is equal to 1.215 for $e_0 = 0.99$ and 1.018 for $e_0 = 0.90$. For less values of t/a the difference between analytical and numerical results become smaller and approach one.

The example of the deflection shape of a porous plate is shown in Annex.

5.2. Buckling of a porous plate

Numerical analysis of buckling of a porous beam was presented in the work of Magnucki and Stasiewicz (2004).

In the considered problem finite elements used for buckling analysis were the same as in the problem of a bending plate. Investigation was done in the ANSYS environment. The eigenvalue and eigenvector problems, which are connected with a buckling analysis, are solved with the use of the subspace method including Jacobi algorithm.

The graphs representing dimensionless critical load $f_{x,CR}^{FEM}$ depending on the ratio a/b of a plate are shown in Fig. 11.

The dimensionless critical load $f_{x,CR}^{FEM}$ is bigger for bigger values of a/b ratio and becomes smaller with the increase of the porosity ratio e_0 . Different porosity coefficients e_0 and ratios of load C_{xy} are considered. Comparison of numerical results $f_{x,CR}^{FEM}$ with analytical ones $f_{x,CR}$ is presented in Fig. 12. The maximum difference between analytical and numerical results does not exceed 0.6% and is largest for $C_{xy} = 2$ and $a/b = 1$.

The example of the buckling shape of a porous plate is shown in Annex.

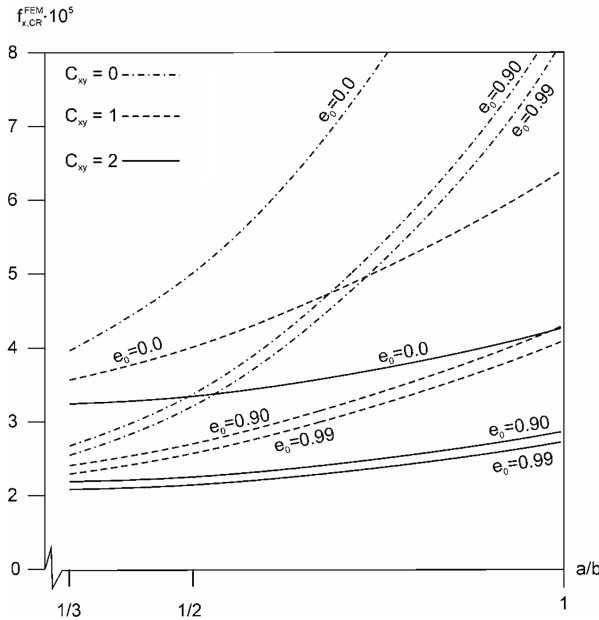


Fig. 11 Dimensionless critical load $f_{x,CR}^{FEM}$ as a function of the ratio a/b

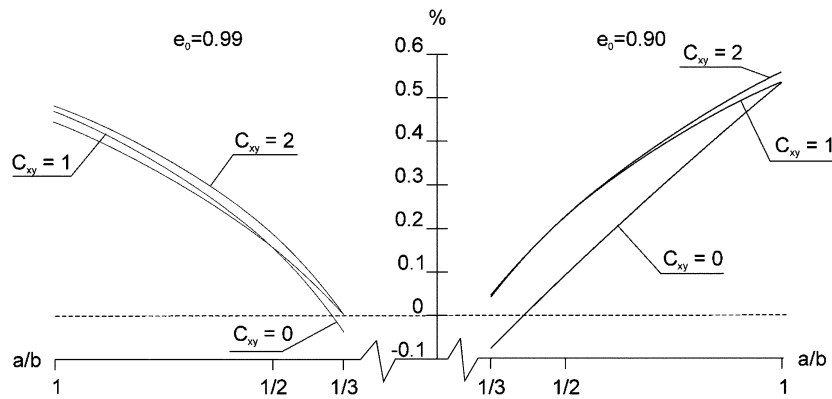


Fig. 12 Relative difference between $f_{x,CR}^{FEM}$ and $f_{x,CR}$ as a function of the ratio a/b

6. Conclusions

The data obtained for considered bending porous plates with a porosity coefficient $e_0 = 0.90, 0.99$ show that differences between maximum normal stresses obtained numerical and analytical are smaller than 12%, whereas differences between relative deflections do not exceed 22%. These differences become even smaller for thinner plates, in other words when a ratio t/a is smaller. They are also smaller for small values of a porosity coefficient. For example, the maximum difference of the relative deflection of a plate with parameters $a/b = 1, t/a = 1/10$ is equal to 1.8%.

In the case of stability of considered porous plates the increase in the porosity of an inner structure causes the value of critical load to become lower. A difference between dimensionless critical loads obtained numerically and analytically does not exceed 0.6% and is the biggest for a square plate ($a/b = 1$). It can be underlined that not only analytical values of buckling load are in agreement with numerical ones but also the buckling shape, i.e., the number of buckling waves $m = 1$ and $n = 1$ for a square plate.

References

- Ambartsumian, S. A. (1987), *Theory of Anisotropic Plates*, Nauka, Moscow (in Russian).
- Banhart, J. (2001), "Manufacture, characterization and application of cellular metals and metal foams", *Progress in Material science*, **46**(6), 559-632.
- Bažant, Z. P. and Cedolin, L. (1991), *Stability of Structures*, Oxford University Press, New York, Oxford.
- Carrera, E. (2000), "An assessment of mixed and classical theories on global and local response of multilayered orthotropic plates", *Composite Structures*, **50**, 183-198.
- Carrera, E. (2001), "Developments, ideas, and evaluations based upon Reissner's mixed variational theorem in the modeling of multilayered plates and shells", *Applied Mechanics Reviews*, **54**(4), 301-329.
- Carrera, E. (2003), "Historical review of Zig-Zag theories for multilayered plates and shells", *Applied Mechanics Reviews*, **56**, 287-308.
- Chattopadhyay, A. and Gu, H. (1996), "Exact elasticity solution for buckling of composite laminates", *Composite Structures*, **34**(3), 291-299.
- Idlbi, A., Karama, M. and Touratier, M. (1997), "Comparison of various laminated plate theories", *Composite Structures*, **37**(2), 173-184.
- Jones, R. M. (1975), *Mechanics of Composite Materials*, McGraw-Hill, Washington.
- Magnucki, K. and Stasiewicz, P. (2004a), "Elastic bending of an isotropic porous beam", *Int. J. Appl. Mech. and Eng.*, **9**(2), 351-360.
- Magnucki, K. and Stasiewicz, P. (2004b), "Elastic buckling of a porous beam", *J. Theoretical and Applied Mechanics*, **42**(4), 859-868.
- Mielniczuk, J. (2000), *Plasticity of Porous Materials. Theory and the Limit Load Capacity*, Poznan University of Technology Publishers, Poznan.
- Noor, A. K., Burton, W. S. and Bert, C. W. (1996), "Computational models for sandwich panels and shells", *Applied Mechanics Reviews*, **49**(3), 155-199.
- Noor, A. K., Malik, M. (2000), "An assessment of five modeling approaches for thermo-mechanical stress analysis of laminated composite panels", *Comput. Mech.*, **25**, 43-58.
- Reddy, J. N., (2004), *Mechanics of Laminated Composite Plates and Shells: Theory and Analysis*, CRC Press.
- Vinson, J. R., (1999), *The Behavior of Sandich Structures of Isotropic and Composite Materials*, Technomic Publishing Company, Inc., Lancaster.
- Wang, C. M., Reddy, J. N. and Lee, K. H. (2000), *Shear Deformable Beams and Plates*, Elsevier: Amstrdam, Lousanne, New York, Oxford, Singapore, Tokyo.
- Wozniak, C. (2001), *Technology Mechanics. Mechanics of Elastic Plates and Shells, Vol. VIII*, Scientific Publishers PWN, Warszawa (in Polish).

Annex

The components of strain state – geometrical relations:

$$\varepsilon_x = \frac{\partial u}{\partial x} = -t \left\{ \zeta \frac{\partial^2 w}{\partial x^2} - \frac{1}{\pi} \left[\frac{\partial \psi_1}{\partial x} \sin(\pi \zeta) + \frac{\partial \psi_2}{\partial x} \sin(2\pi \zeta) \cos^2(\pi \zeta) \right] \right\} \quad (\text{A1})$$

$$\varepsilon_y = \frac{\partial v}{\partial y} = -t \left\{ \zeta \frac{\partial^2 w}{\partial y^2} - \frac{1}{\pi} \left[\frac{\partial \phi_1}{\partial y} \sin(\pi \zeta) + \frac{\partial \phi_2}{\partial y} \sin(2\pi \zeta) \cos^2(\pi \zeta) \right] \right\} \quad (\text{A2})$$

$$\gamma_{xy} = \frac{\partial u}{\partial y} + \frac{\partial v}{\partial x} = -t \left\{ 2\zeta \frac{\partial^2 w}{\partial x \partial y} - \frac{1}{\pi} \left[\left(\frac{\partial \psi_1}{\partial y} + \frac{\partial \phi_1}{\partial x} \right) \sin(\pi \zeta) + \left(\frac{\partial \psi_2}{\partial y} + \frac{\partial \phi_2}{\partial x} \right) \sin(2\pi \zeta) \cos^2(\pi \zeta) \right] \right\} \quad (\text{A3})$$

$$\gamma_{xz} = \frac{\partial u}{\partial z} + \frac{\partial w}{\partial x} = \psi_1(x, y) \cos(\pi \zeta) + \psi_2(x, y) [\cos(2\pi \zeta) + \cos(4\pi \zeta)] \quad (\text{A4})$$

$$\gamma_{yx} = \frac{\partial v}{\partial z} + \frac{\partial w}{\partial x} = \phi_1(x, y) \cos(\pi \zeta) + \phi_2(x, y) [\cos(2\pi \zeta) + \cos(4\pi \zeta)] \quad (\text{A5})$$

The stiffness coefficients of a porous plate

$$C_1 = \frac{1}{12} \left(1 - 6 \frac{\pi^2 - 8}{\pi^3} e_0 \right), \quad C_2 = \frac{1}{\pi^2} \left(\frac{2}{\pi} - \frac{1}{e} e_0 \right), \quad C_3 = \frac{1}{\pi^2} \left(\frac{3}{16} - \frac{32}{75\pi} e_0 \right),$$

$$C_4 = \frac{1}{\pi^2} \left(\frac{1}{2} - \frac{2}{3\pi} e_0 \right), \quad C_5 = \frac{1}{\pi^2} \left(\frac{8}{15\pi} - \frac{1}{8} e_0 \right), \quad C_6 = \frac{1}{\pi^2} \left(\frac{5}{32} - \frac{128}{315\pi} e_0 \right),$$

$$C_7 = \frac{1}{2} - \frac{4}{3\pi} e_0, \quad C_8 = \frac{8}{15\pi} - \frac{1}{4} e_0, \quad C_9 = 1 - \frac{832}{315\pi} e_0$$

The coefficients of shear functions

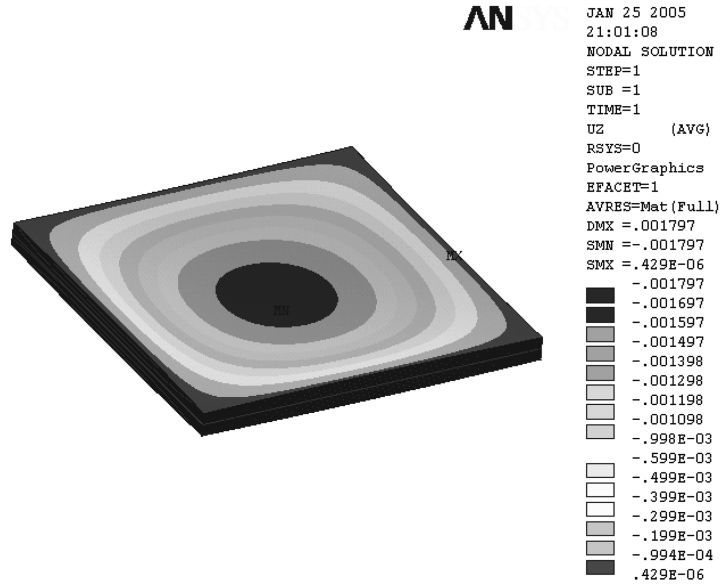
$$\alpha_1 = \frac{a_{22}b_1 - a_{12}b_2}{a_{11}a_{22} - a_{12}^2}, \quad \beta_1 = \frac{a_{11}b_2 - a_{21}b_1}{a_{11}a_{22} - a_{12}^2}$$

$$a_{11} = (C_4 + C_5 C_{10}) \left[1 + \frac{1-\nu}{2} \left(\frac{na}{mb} \right)^2 \right] \left(m\pi \frac{t}{a} \right)^2 + \frac{1-\nu}{2} (C_7 + C_8 C_{10}),$$

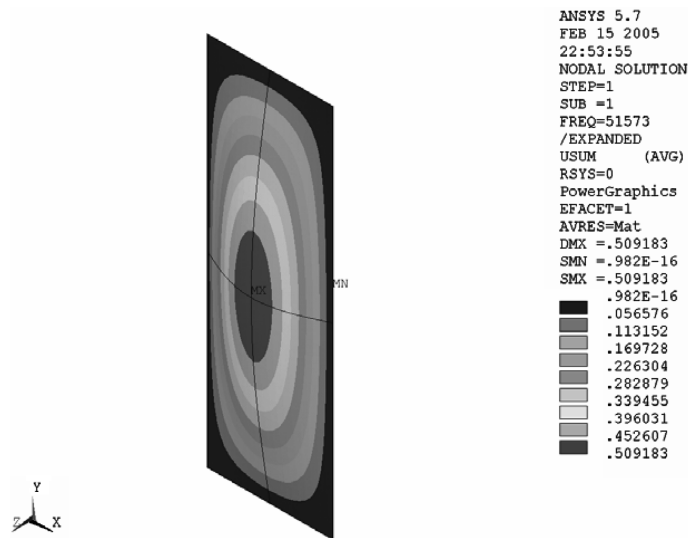
$$a_{12} = \frac{1+\nu}{2} (C_4 + C_5 C_{10}) mn\pi^2 \frac{t^2}{ab}$$

$$a_{22} = (C_4 + C_5 C_{10}) \left[\frac{1-\nu}{2} + \left(\frac{na}{mb} \right)^2 \right] \left(m\pi \frac{t}{a} \right)^2 + \frac{1-\nu}{2} (C_7 + C_8 C_{10})$$

$$b_1 = C_2 \left[1 + \left(\frac{na}{mb} \right)^2 \right] \left(m\pi \frac{t}{a} \right)^3, \quad b_2 = C_2 \left[1 + \left(\frac{na}{mb} \right)^2 \right] m^2 n\pi^3 \frac{t^3}{a^2 b}$$



Example of deflection of a porous plate w_a^{FEM} [m] ($e_0 = 0.9$, $a/b = 1$, $t/a = 1/15$, $p_0 = 1$ MPa)



Example of buckling of a porous plate ($e_0 = 0.99$, $C_{xy} = 1$, $a/b = 1/3$, $t/a = 1/160$)